Letter Vol. 49, No. 1 / 1 January 2024 / Optics Letters 41

Unified framework for terahertz radiation from a single- or two-color plasma filament

Feifan Zhu,[1] Jiayu Zhao,[1,*] Li Lao,[2] Yan Peng,[1,3] and Yiming Zhu[1,3]

[1]Terahertz Technology Innovation Research Institute, Terahertz Spectrum and Imaging Technology Cooperative Innovation Center, Shanghai Key Lab of Modern Optical System, University of Shanghai for Science and Technology, Shanghai 200093, China
[2]Tera Aurora Electro-optics Technology Co., Ltd., Shanghai 200093, China
[3]Shanghai Institute of Intelligent Science and Technology, Tongji University, Shanghai 200092, China
*zhaojiayu@usst.edu.cn

Received 21 June 2023; revised 25 October 2023; accepted 27 October 2023; posted 9 November 2023; published 19 December 2023

The plasma filament induced by photo-ionization in transparent media (e.g., air) is a competitive terahertz (THz) source, whose mechanism has been widely studied in two separate schemes, i.e., the one- or two-color femtosecond laser filamentation. However, the physical commonality of these two schemes is less explored currently, and a common theory is in urgent need. Here, we proposed the traveling-wave antenna (TWA) model applicable to both single- and dual-color laser fields, which successfully reproduced the reported far-field THz angular distribution/dispersion from different filament lengths with either a constant or a varied plasma density. This work paves the way toward a deeper understanding of the important laser-filament-based THz sources within the same theoretical framework.

https://doi.org/10.1364/OL.498603

Introduction. Over the past two decades, terahertz (THz) technology has received significant attention and undergone rapid developments. For example, multiple choices have emerged for THz sources, including quantum cascade lasers [1], photoconductive antennas [2], laser-pumping nonlinear crystals [3], laser ionization of solids [4], or transparent media (e.g., air) [5–8]. Among these options, the air plasma during femtosecond laser filamentation is an important THz source combining broad bandwidth and high intensity [9,10]. Thus, the underlying mechanism has become a hot topic in the community, and efforts have been made on two typical schemes, namely, the single- [11,12] and dual-color photoionization [13–16]. Since these two fields are normally considered to be governed by completely different mechanisms, as a result, physical models were established, separately, to explain the experimental phenomena in each field [11,12] versus [5,13,14,17,18].

However in recent times, a new requirement has been raised for a unified picture or framework that can provide a clue for systematically summarizing a set of major experimental observations from the two fields, in order to gain a deeper understanding of the physical commonality. Therefore, there have been works recently for both one- and two-color laser excitations of THz wave generation, e.g., a combined model applied for the THz aqueous photonics [19] and an antenna model working for the microwave-to-THz radiation from the air plasma [20,21]. Nevertheless, the former theory mainly focused on the ionization medium of water, leaving blanks for the fundamental gas case, and the latter stressed mostly on the microwave phenomenon (<0.05 THz). More importantly, contributions of the crucial relative phase between the fundamental light and its second harmonic in the two-color condition were not sufficiently studied therein [20,21].

In order to resolve the above issues, here we proposed a unified framework of the traveling-wave antenna (TWA) concept with potential to bridge the single- and dual-color fields. Briefly, a simple phase factor has been added into the traditional TWA modal equation borrowed from the microwave photonics, which could account for the relative phase between the pumping laser and its second harmonic in case of two-color laser pumping. Afterward, we concentrated on the THz angular distribution/dispersion from different dual-color plasma filament lengths, as a function of which, the phase effect has been investigated. Meanwhile, the plasma density was also carefully treated to be either changed with the filament length or remained as a constant. Accordingly, the suggested TWA model effectively reproduced representative results reported in the literature. Moreover, when considering the infinite dephasing length within the phase factor toward the single-color case, the reworked TWA modal formula can be easily restored to its origin form, which has been recently proved by us to be applicable to the single-color field with a comprehensive reproduction of the far-field THz radiation patterns from the air/water plasma filament(s) [22]. Therefore, this work has successfully included both the single- and two-color plasma-filament-based THz generations inside the same TWA frame, by which means the unified understanding is achieved.

Framework of the TWA concept. In microwave photonics, antennas with current distributions represented by traveling waves in the same direction are referred to as traveling-wave antennas (TWA). The corresponding TWA model describes electromagnetic (EM) radiations from this antenna [20,23]:

$$E(\omega,\theta,l)=\left|\frac{\eta}{2\pi r}\cdot j_0(\omega)\sin\theta\cdot Q(\omega,\theta,l)\right|. \quad (1)$$

In the laser plasma region, THz emissions during single-color laser filamentation can also be interpreted by this model as we

demonstrated in Ref. [22]. In this situation, two building blocks of the THz–TWA model, namely, the element and space factors, can be learned from Eq. (1). Firstly, the current element factor indicates the type of current and its direction of flow as $j_0(\omega)\sin\theta$, where $j_0(\omega)$ is the spectral current [14,22] and ω is the THz angular frequency with θ defined as the angle relative to the current axis (z). Secondly, the space factor provides an accurate description of the phase matching condition as $Q(\omega,\theta,l)=\frac{\sin[(kl/2)(K-\cos\theta)]}{(K-\cos\theta)}$, where $k=\omega/c$ is the THz wave number in free space, l is the filament length, and K indicates the ratio between the THz phase velocity and the laser group velocity, i.e., the walk-off effect. Besides, r is for the polar coordinate and η is the intrinsic impedance.

When switching from the single- to two-color filamentation, the relative phase difference (ϕ) between the fundamental laser and its second harmonic is a non-negligible parameter, because the generated THz properties were strongly affected by ϕ when it was modulated either by adjusting the BBO-to-focus distance or by changing the filament length, etc. In view of this point, a phase factor has been added into the modal equation. Briefly, we first recalled the un-integrated appearance of Eq. (1) as Eq. (2):

$$E(\omega,\theta,l)=i\eta\frac{k\exp(-ikr)}{4\pi r}\sin\theta\int_{-l/2}^{l/2}j_0(\omega)\exp(ikz\cos\theta-ik'z)dz, \tag{2}$$

where k' is the wave number of the driven laser. Then, the ϕ factor was inserted into this monochromatic TWA formula in form of $\sin\phi$ [18,24], and the re-worked TWA model for the two-color case is

$$E(\omega,\theta,l,\phi)\propto i\eta\frac{k\exp(-ikr)}{4\pi r}\sin\theta\cdot\int_{-l/2}^{l/2}j_0(\omega)\cdot\sin\phi\cdot\exp(ikz\cos\theta-ik'z)dz, \tag{3}$$

where $\phi=\phi_0+k_dl$ with ϕ_0 as the initial phase determined by the frequency doubling process and $k_d=\pi/l_d$ as the dephasing wave number. Specifically, l_d is the dephasing length [18] over which the two colors' phase difference will slip by π and can be estimated by $l_d=(\lambda_{laser}/2)/\Delta n$. Here, λ_{laser} is the wavelength of the fundamental laser, and Δn is the refractive index difference between the fundamental laser and its second harmonic, contributed from both air and plasma dispersion. That is, $\Delta n=\Delta n_{\rm air}+\Delta n_{\rm plasma}$, with $n_{\rm air}$ defined in Ref. [25], $n_{\rm plasma}=(1-\omega_p{}^2/\omega^2)^{1/2}$ and $\omega_p=(e^2N_e/m_e\varepsilon_0)^{1/2}$. Here, we could consider a Gaussian/constant N_e distribution along the laser filament. While for the transverse scale, it is neglectable since the studied THz wavelengths are normally larger than the filament diameter. After integrations, Eq. (3) is finally written as

$$E(\omega,\theta,l,\phi_0)\propto i\exp(-ikr)\frac{\eta}{4\pi r}\cdot j_0(\omega)\sin\theta\cdot\left[e^{i\phi_0}\frac{\sin[(\frac{kl}{2})(K-\cos\theta-\frac{\lambda}{2l_d})]}{(K-\cos\theta-\frac{\lambda}{2l_d})}-e^{-i\phi_0}\frac{\sin[(\frac{kl}{2})(K-\cos\theta+\frac{\lambda}{2l_d})]}{(K-\cos\theta+\frac{\lambda}{2l_d})}\right]. \tag{4}$$

In this two-color-field formula, the dephasing length l_d is a representative new parameter. One can predict by $l_d\propto 1/\Delta n$ that l_d would be larger when the two laser frequency components (f_1 versus f_2) have a smaller Δf and thus a smaller Δn. Following this clue, l_d would approach infinite if "$f_1=f_2$" and "$\Delta n=0$" were allowed. In this case, by setting l_d as ∞, Eq. (4) can be simplified into Eq. (1), indeed, the single-color case. Therefore,

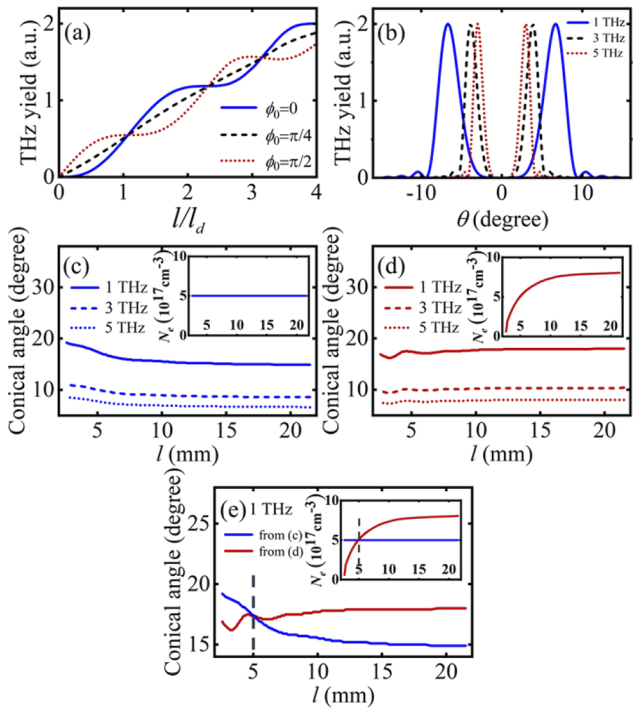

Fig. 1. Calculations by the TWA model. (a) THz yields with the increasing filament lengths at $\phi_0=0$, $\pi/4$, and $\pi/2$. (b) Far-field THz angular distributions at 1, 3, and 5 THz. (c)–(d) Conical angles of the THz radiation as a function of the filament length at 1, 3, and 5 THz in condition of N_e being kept constant (c) or being varied (d). (e) N_e evolutions and corresponding conical angles at 1 THz, extracted from (c) and (d) for better comparison.

Eq. (4) is actually the general formula for the TWA concept connecting the two different domains of single- and two-color fields. In the next section, Eq. (4) would be tested with three parameters (ϕ_0, ω, and l_d) being varied.

Investigation of the TWA model via key parameters. *THz yields with different initial phases* (ϕ_0). The first demonstration of the TWA formula [Eq. (4)] is by means of predicting the THz yield under different ϕ_0. Setting 1 THz as an example, the THz yield over the 360° ($\int_{-\pi}^{\pi}|E(\theta,l,\phi_0)|^2d\theta$) was calculated from a length-varied filament with a constant l_d~22 mm for 800 nm and 400 nm laser inside the N_e~10^{16} cm^{-3} plasma [18] but with different initial ϕ_0 of 0, π/4, and π/2, respectively. The calculation results are shown in Fig. 1(a), inside which the THz yield with $\phi_0=\pi/4$ increased almost linearly, while those at $\phi_0=0$ and $\phi_0=\pi/2$ grew in steps around that at π/4. This indicates that the initial phase does not change the overall trend of THz enhancement with the increasing filament length but only has a periodic fluctuating effect. These phenomena have also been observed in Refs. [18,24], validating our TWA method. If the THz-laser walk-off effect is further enhanced, the saturation of THz output can be observed [5] (Section A of Supplement 1).

Far-field angular distributions at different THz frequencies (ω). Frequency-dependent THz angular distributions have drawn intense attention for studying the laser-filament-based THz sources [5,15,18,24,26]. Here, we also calculated the far-field THz angular dispersion $|E(\omega,l)|^2$ at three frequencies (1, 3, and 5 THz) with N_e~1×10^{16} cm^{-3}, l_d~22 mm and $l=2l_d$. As shown in

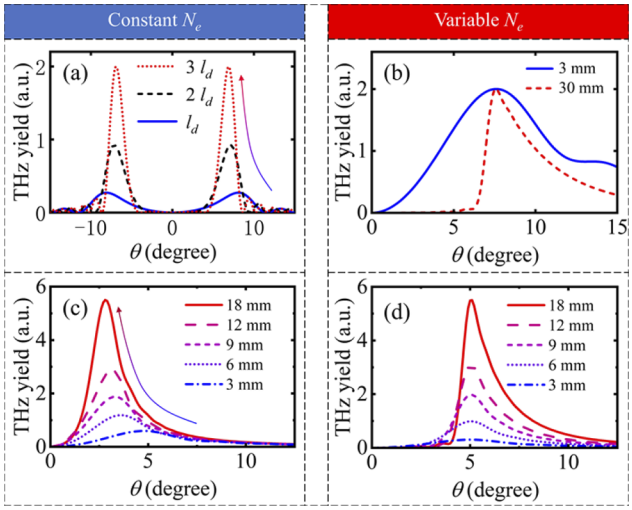

Fig. 2. TWA-based calculations of far-field THz angular distributions with a constant or variable N_e. (a) For filament lengths of $l = l_d$, $2l_d$, and $3l_d$ at 1 THz, following Ref. [18]. (b) For $l = 3$ and 30 mm over 0.1–4 THz, following Ref. [5]. (c)–(d) For $l = 3$, 6, 9, 12, and 18 mm over 0.5–15 THz, following Ref. [24].

Fig. 1(b), typical conical THz emissions were observed, and the angular dispersion properties are exactly the same with Ref. [18] that the conical angle gradually decreased from 7° to 3° as the frequency increased from 1 to 5 THz. Moreover, compared with Ref. [18], our TWA theory succeeds by the reproduction of the angular distribution with filaments shorter than the dephasing length l_d. This point will be discussed in Fig. 2.

Conical angles of the THz radiation in case of (in)variable dephasing length (l_d). In this section, we studied the effect of l_d on THz generation by changing the plasma density (N_e), which crucially decides the l_d value as interpreted earlier. For laser plasma filaments, it is possible to maintain the N_e value when enhancing the pumping laser power and the filament length, e.g., by tilting the focusing lens [24], while the most common case is that N_e increases with the filament length while approaching saturated. Both of the above situations have been considered by us.

For the former case, we assume that different lengths of laser filaments are all set with a constant N_e as $5 \times 10^{17}\,\mathrm{cm}^{-3}$ (l_d~4.6 mm). In this case, the laser filament is similar to a basic metal antenna, whose length can be varied while N_e is fixed. It is well known that the radiation angle of such a metal antenna decreases as the length increases. This is actually what can be found in the TWA calculation results as shown in Fig. 1(c), where the conical angles of THz emissions retrieved from $|E(\omega,l)|^2$ at 1, 3, and 5 THz decreased from 19° to 15°, 11° to 8.6°, and 8.6° to 6.6°, respectively, as the filament length increased from 3 to 20 mm.

For the other case of a varied N_e (between 5×10^{16} and $1 \times 10^{18}\,\mathrm{cm}^{-3}$ (in Section B in Supplement 1), corresponding $l_d = 16$ to 3 mm) with respect to the filament length; however, all conical THz angles roughly remained the same as shown in Fig. 1(d). This special phenomenon can be understood as follows. We extracted the N_e distributions and corresponding 1 THz results from Figs. 1(c) and 1(d) into Fig. 1(e). Then, one can see in the inset of Fig. 1(e) that when l is shorter than 5 mm, the N_e value from Fig. 1(d) as the red line is smaller than that from Fig. 1(c) as the blue line. Considering that inside a low-N_e environment, Δn between the fundamental laser and its second harmonic is also little, this would result in a large l_d, which further leads to a small conical angle [18]. Thus in Fig. 1(e) for the conical angle before $l = 5$ mm, the values from Fig. 1(d) (red line) are as expected smaller than that from Fig. 1(c) (blue line). While after $l = 5$ mm, the situation is the exact opposite and the red line is above the blue one. Furthermore, due to the decreasing profile of the blue line, the red line exhibits a relatively horizontal style as shown in Figs. 1(d) and 1(e). In order to further verify our TWA model based on the above two N_e conditions, we reproduced results in the literature in the next section.

Reproductions of representative reports in the literature. Comparisons have been carried out between the TWA outcomes and three highly cited publications, whose theories about the THz profiles detected in the far field are widely accepted. Firstly, Ref. [18] focused on THz angular distributions from a two-color laser filament by using the famous off-axis phase matching model. Secondly, Ref. [5] proposed a successful physical model based on a linear dipole array along the two-color laser filament for describing the conical THz radiation. Thirdly, Ref. [24] reproduced the THz angular results from both its experiments and existing publications by considering comprehensive parameters during dual-color laser filamentation. These three works are divided into two categories for our reproductions and comparisons with N_e being kept either constant or varied, as shown in Fig. 2.

In Fig. 2(a), THz angular distributions $|E(\theta,l)|^2$ were calculated according to the parameters in Ref. [18], i.e., at 1 THz and $l = l_d$, $2l_d$, and $3l_d$, respectively, where $l_d = 22$ mm. Here, since l_d was fixed, the corresponding N_e could only be treated as an invariant parameter regardless of the filament length l. It can be seen that the resultant THz conical angles decreased from 8.2° to 6.9° as l increased, whose variation trend is quantitatively the same with Ref. [18] (see also Section C of Supplement 1). However, it is worth noting that the off-axis phase-matching model in Ref. [18] cannot well display the conical THz radiation profile from short filaments (such as $l = l_d$), as shown in Section C of Supplement 1 as an on-axis pattern rather than a conical one. This issue could be attributed to the neglect of the in-filament THz phase change required for establishing conical emissions [24]. Please see also Section D of Supplement 1 for the mechanisms' transition from short to long filaments [24]. While for our TWA model, it is applicable for both the cases of $l <= l_d$ and $l > l_d$, as displayed in Fig. 2(a) and Figs. 2(b)–2(d).

In Fig. 2(b), N_e was designed to be changed with the filament length as the latter was scanned by a metal iris along the longitudinal direction as did in Ref. [5]. This time, both short and long filaments ($l = 3$ and 30 mm) have been studied with N_e estimated as 5×10^{16} and $8 \times 10^{17}\,\mathrm{cm}^{-3}$ [inset of Fig. 1(d)], and the corresponding THz angular distributions were calculated in a broadband within 0.1–4 THz. It can be seen in Fig. 2(b) that conical angles of the THz radiation are almost the same at about 7.5°, which are independent of the filament lengths. Moreover, the lobewidth of THz emission from the 30 mm filament is much less than that from the 3 mm one given by the TWA model. These observations agree with Ref. [5]. For reasons of the sharp edge in Fig. 2(b), please see Sections E and F of Supplement 1.

At last in Figs. 2(c) and 2(d), both conditions of constant and variable N_e have been considered for the angle-dependent THz yields over 0.5–15 THz from different filament lengths (3, 6, 9, 12, and 18 mm) by adopting the parameters in Ref.

[24]. It can be seen that the reference's results (Section G in Supplement 1) can be well reproduced by the TWA model in both cases. Specifically, as shown in Fig. 2(c), when N_e is fixed as $1\times10^{17}\,\mathrm{cm}^{-3}$ ($l_d = 13.3$ mm), the conical THz angle gradually decreased from 5 to 2.5, as the filament length increased. By contrast in Fig. 2(d), when N_e varied between 5×10^{16} and $1\times10^{18}\,\mathrm{cm}^{-3}$ with the growth of filament lengths, the conical THz angle remained at around 5°.

By comparison with the above works, the TWA model has been verified. It is worth mentioning that a weak on-axis THz radiation can also be experimentally detected and reproduced by the TWA model (Section H of Supplement 1). More importantly, this model has bridged both domains of single- and two-color fields with a simple transform from Eq. (4) to Eq. (1) by reasonably omitting only the l_d effect as discussed in Section 2. Then, Eq. (1) can be fully applied in the single-color field as performed in Ref. [22].

Conclusion. In summary, the proposed frame of TWA concept in this work possesses the ability of accounting for THz waves generation during both single- and two-color femtosecond laser filamentation. Modal formulas for the two cases [Eq. (1) and Eq. (4)] are bridged by a simple phase factor considering the relative phase difference between the fundamental laser and its second harmonic. Representative far-field THz profiles in two cases can be accurately described by the same TWA theory. Specifically, characteristics of the THz angular distribution/dispersion have been investigated, which indicated a strong dependence on relationships between the plasma density and the filament length (Fig. 1). Key results in highly cited publications [5,18,24] have been efficiently reproduced (Fig. 2), verifying the TWA model.

In future works, this model could not only promote unified understanding of the two important fields in terms of far-field THz patterns but also would be able to interpret more natures of THz radiations from filaments, such as waveform, polarization, and bandwidth, if equipped with the time–domain analysis [20,22,27–30]. Moreover, our theory is promising to serve a wide region of pumping schemes, e.g., the three- or multi-color-laser-based THz creations with improved phase factors, and might also be extended to filament-driven sources beyond THz bands.

Funding. National Natural Science Foundation of China (61988102, 62335012); Youth Sci-Tech "Qimingxing" Program of Shanghai (22QC1400300); National Key Research and Development Program of China (2022YFA1404004).

Disclosures. The authors declare no conflicts of interest.

Data availability. Data underlying the results presented in this paper are not publicly available at this time but may be obtained from the authors upon reasonable request.

Supplemental document. See Supplement 1 for supporting content.

REFERENCES

1. A. Khalatpour, A. K. Paulsen, C. Deimert, Z. R. Wasilewski, and Q. Hu, Nat. Photonics **15**, 16 (2021).
2. X. Ropagnol, Z. Kovács, B. Gilicze, M. Zhuldybina, F. Blanchard, C. M. Garcia-Rosas, S. Szatmári, I. B. Földes, and T. Ozaki, New J. Phys. **21**, 113042 (2019).
3. B. Zhang, Z. Ma, J. Ma, X. Wu, C. Ouyang, D. Kong, T. Hong, X. Wang, P. Yang, L. Chen, Y. Li, and J. Zhang, Laser Photonics Rev. **15**, 2000295 (2021).
4. G. Liao, Y. Li, H. Liu, G. G. Scott, D. Neely, Y. Zhang, B. Zhu, Z. Zhang, C. Armstrong, E. Zemaityte, P. Bradford, P. G. Huggard, D. R. Rusby, P. McKenna, C. M. Brenner, N. C. Woolsey, W. Wang, Z. Sheng, and J. Zhang, Proc. Natl. Acad. Sci. U. S. A. **116**, 3994 (2019).
5. Z. Zhang, Y. Chen, M. Chen, Z. Zhang, J. Yu, Z. Sheng, and J. Zhang, Phys. Rev. Lett. **117**, 243901 (2016).
6. L. Zhang, W. Wang, T. Wu, S. Feng, K. Kang, C. Zhang, Y. Zhang, Y. Li, Z. Sheng, and X. Zhang, Phys. Rev. Appl. **12**, 014005 (2019).
7. A. D. Koulouklidis, C. Gollner, V. Shumakova, V. Y. Fedorov, A. Pugžlys, A. Baltuška, and S. Tzortzakis, Nat. Commun. **11**, 292 (2020).
8. A. V. Balakin, J. L. Coutaz, V. A. Makarov, I. A. Kotelnikov, Y. Peng, P. M. Solyankin, Y. Zhu, and A. P. Shkurinov, Photonics Res. **7**, 678 (2019).
9. H. G. Roskos, M. D. Thomson, M. Kreß, and T. Löffler, Laser Photonics Rev. **1**, 349 (2007).
10. M. Clerici, M. Peccianti, B. E. Schmidt, L. Caspani, M. Shalaby, M. Giguere, A. Lotti, A. Couairon, F. Legare, T. Ozaki, D. Faccio, and R. Morandotti, Phys. Rev. Lett. **110**, 253901 (2013).
11. H. Hamster, A. Sullivan, S. Gordon, W. White, and R. W. Falcone, Phys. Rev. Lett. **71**, 2725 (1993).
12. C. D'Amico, A. Houard, M. Franco, B. Prade, A. Mysyrowicz, A. Couairon, and V. T. Tikhonchuk, Phys. Rev. Lett. **98**, 235002 (2007).
13. D. J. Cook and R. M. Hochstrasser, Opt. Lett. **25**, 1210 (2000).
14. K. Y. Kim, J. H. Glownia, A. J. Taylor, and G. Rodriguez, Opt. Express **15**, 4577 (2007).
15. V. A. Andreeva, O. G. Kosareva, N. A. Panov, D. E. Shipilo, P. M. Solyankin, M. N. Esaulkov, P. González de Alaiza Martínez, A. P. Shkurinov, V. A. Makarov, L. Bergé, and S. L. Chin, Phys. Rev. Lett. **116**, 063902 (2016).
16. J. Y. Zhao, W. W. Liu, S. C. Li, D. Lu, Y. Z. Zhang, Y. Peng, Y. M. Zhu, and S. L. Zhuang, Photonics Res. **6**, 296 (2018).
17. N. Karpowicz and X. C. Zhang, Phys. Rev. Lett. **102**, 093001 (2009).
18. Y. S. You, T. I. Oh, and K. Y. Kim, Phys. Rev. Lett. **109**, 183902 (2012).
19. H. Y. Wang and T. Shen, Appl. Phys. Lett. **117**, 131101 (2020).
20. A. M. Zheltikov, Opt. Lett. **46**, 4984 (2021).
21. A. V. Mitrofanov, D. A. Sidorov-Biryukov, M. V. Rozhko, N. V. Erukhimova, A. A. Voronin, M. M. Nazarov, A. B. Fedotov, and A. M. Zheltikov, Phys. Rev. A **105**, 053503 (2022).
22. J. Y. Zhao, Q. N. Wang, Y. C. Hui, Y. M. Chen, F. F. Zhu, Z. M. Jin, A. P. Shkurinov, Y. Peng, Y. M. Zhu, S. L. Zhuang, and L. Lao, SciPost Phys. Core **5**, 046 (2022).
23. C. Balanis, *Antenna Theory Analysis and Design*, (Wiley & Sons, 2005).
24. A. Gorodetsky, A. D. Koulouklidis, M. Massaouti, and S. Tzortzakis, Phys. Rev. A **89**, 033838 (2014).
25. B. Edlén, Metrologia **2**, 71 (1966).
26. J. Y. Zhao, W. Chu, Z. Wang, Y. Peng, C. Gong, L. Lin, Y. M. Zhu, W. W. Liu, Y. Cheng, S. L. Zhuang, and Z. Z. Xu, ACS Photonics **3**, 2338 (2016).
27. Y. M. Chen and J. Y. Zhao, Results Phys. **15**, 102577 (2019).
28. Y. Peng, J. L. Huang, J. Luo, Z. F. Yang, L. P. Wang, X. Wu, X. F. Zang, C. Yu, M. Gu, Q. Hu, X. C. Zhang, Y. M. Zhu, and S. L. Zhuang, Photonis X **2**, 12 (2021).
29. Y. Zhu, X. F. Zang, H. X. Chi, Y. W. Zhou, Y. M. Zhu, and S. L. Zhuang, Light: Adv. Manufact. **4**, 1 (2023).
30. X. F. Zang, B. S. Yao, L. Chen, J. Y. Xie, X. G. Guo, A. V. Balakin, A. P. Shkurinov, and S. L. Zhuang, Light: Adv. Manufact. **2**, 148 (2021).